

# Four-bar Linkage Transformable Wheels

**Group 14:** Ren Xuesong, Chen Rui, Teng Muwei, Lu Changqing

**Abstract**—Vehicles that can travel through complicated surface are needed in many fields nowadays. Transformable wheel is a solution to allow vehicles transform wheels shape to accommodate the different surfaces or to overcome obstacles. In this project, we simulate different situations that vehicles may encounter, including a 6cm height step(obstacles), sand(desert) and concrete land(road), 10cm height gate(tunnels). A six-teethed transformable wheel is designed to make the vehicle climb or pass through the obstacles stably and fast. The design is based on special case III four-bar linkage, transforming angular displacement into change in diameters of wheels. The diameter of wheel in shrink mode is 86mm, while in expand mode, the diameter becomes 140mm. The maximum torque required to expand the wheel and to overcome its self weight is 3.5 kg·cm, which is less than the maximum torque output of the driven servo. The practicability of this design is finally verified by both theory and practice. Besides, we find that based on this design, the maximum torque required increases first and then decreases as the increase of the number of teeth. Methods including changing the number of teeth and moving the barycenter backwards are useful for improving the performance of transformable wheels.

**Index Terms**—Transformable Wheels, Four-bar Linkage

## I. INTRODUCTION

### A. Nature of the Problem

VEHICLES that can travel through terrains of complicated surface shapes can be applied into many cases nowadays such that the speed of relevant operations such as field searching can be increased due to the applications of such vehicles.

In general, the difficulties for modern and conventional vehicles to travel through complicated surfaces lie in that the circular and fixed shape of the wheels can easily run into obstacles that they cannot overcome.

Therefore, one way to solve the problem and to let the vehicles travel with less difficulty is to make the wheels transformable according to the possible obstacles.

### B. Relevant Literature

There are already many studies and designs in this relevant field. Before designing the transformable system, we studied some existing designs for their originality

and potential issues. See Appendix A for more literature review.

For wheels to transform, spacial mechanisms are studied. Some of the work makes use of conventional mechanical linkage system such as slider-crank mechanism [3]. This slider-crank mechanism enables the wheel transform from a circular shape into wheels with spoke while one passive leg taking the load of the vehicle. After transformation, the passive leg will be transformed through a elastic mechanism when rolling to the upper part of the wheel. This passive leg design largely decreases the actuation force of the transformation since when transforming without a passive leg, the spoked structure will require larger force to lift the whole vehicle. However, this requires the vehicle to be able to identify the exact position to transform, which is the position where the passive leg supports the vehicle. This can be a problem since it is hard to predict the position where the passive leg supports the vehicle without using sensors in practice.

Another design uses pin-slot linkage [4] to realize the transformation. Three pin-slot linkages, separated  $120^\circ$  apart, enables three legs to retract in the circular wheel or to stretch out to form a transformed legged wheel. But it remains difficult to control the phases of two wheel during wheel transformation. Since only three legs are stretched out, the vehicle can be easily tilted laterally when the legs on both sides are not in phase.

Other literature explores complicated structures such as origami structures [1] to transform the wheel. This design introduces new ideas other than conventional mechanical structures. New materials can be applied as well because the complicated structure need to be flexible enough to deform. The origami structure applied is called the *magic-ball* structure which can shrink easily to fit the height limitation such as a tunnel. However, the wheel still stays in a circular shape and cannot overcome elevated surfaces such as steps.

To achieve a successful design requires detailed analysis as well. For a spoke wheel structure, a model is established to analyze the motion of straight-line or turning motion of the wheel [2]. The motion analysis suggests sudden accelerations will be generated due to the discontinuity motion of the spoke wheel.

Based on the analysis of the previous work, we can

also predict certain problems such as a relative high actuation force of transformation due to mechanism design. One solution is the passive leg structure. Another solution is to use soft pneumatic actuators [5] while the effect of buckling in the actuators cannot be predicted.

### C. Proposed Design

The design we proposed is a transformation mechanism based on a four-bar linkage system. The CAD drawings are shown in Figure 1a for shrink mode and in Figure 1b for expand mode.

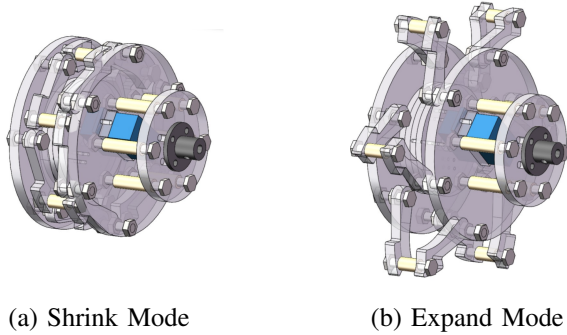


Figure 1: Transformable Wheels: *Transformation is realized by turning the inner circular plate and changing the four-bar linkage system into expand mode such that the six identical linkages are stretched out to form six spoke legs.*

The transformation is completed by rotating the inner circular plate of the wheel to actuate the six identical four-bar linkage to expand the six-spoke structure. The torque required to rotate the inner circular plate is provided by a servo that is assembled in the center of the wheel. The detailed linkage motion analysis and force analysis will be provided in the following section.

When the prototype was completed and tested on a field consists of an elevated step, a tunnel and a sandy surface, the transformation mechanism was proved to be effective. The vehicle can overcome the elevated step, can travel on sandy surface and can travel through the tunnel. Therefore, the proposed design is proved to be valid.

## II. SYNTHESIS

### A. Originality of the Design

This design is based on spacial case III four-bar linkage, which is considered as unstable because of the existence of change point. We limit the input angle so that change point won't occur. What we want to take use of is the symmetrical characteristic of the spacial case III four-bar linkage.

The driven servo is installed inside the wheels. The direct touch makes the system more stable because no conduction structure is needed. We use slide ring to handle the problem of wire arrangement. Hence, the wires of the servo in wheels will not rotate together with the wheel.

MPU6050 Model is used in our design. We utilized pitch of MPU6050 Model to detect whether the vehicle has climbed on the sand box and whether the vehicle has run off the sand box. If pitch is larger than 20, the vehicle has climbed on the sand box. If pitch is smaller than 20, the vehicle has climbed off the sand box. When the vehicle has run off the sand box, the wheels transform from the expansion mode to the shrink mode.

### B. Graphical Linkage Synthesis

1) *Two Position Synthesis:* Since the wheel has two modes: shrink mode and expand mode. By constraining two extreme position of the linkage, we can use two position synthesis to design a valid four-bar linkage system.

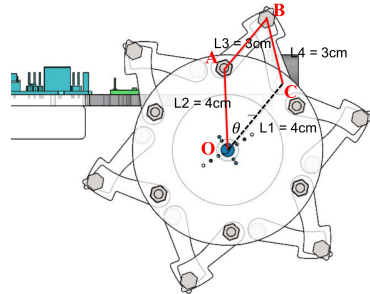


Figure 2: Four-bar Linkage Dimension

As we can see from Figure 2, the input linkage  $L_2$  has a dimension of  $4\text{ cm}$ , and the coupler and output linkage  $L_3$  and  $L_4$  have dimensions of  $3\text{ cm}$ . Point  $B$  is the contacting point when the wheel is in expand mode. And the effective radius of the wheel is the distance between point  $O$  and  $B$ . Therefore, the effective radius in expand mode should be  $R_{expand} = 70\text{ mm}$ . Since when in shrink mode, point  $B$  should not be in contact with the ground so that the wheels remain circular shape. Therefore, when in shrink mode,  $R_{shrink} = 40\text{ mm}$ . By controlling the  $\theta$  in the linkage system using a servo, we can achieve these two extreme positions.

2) *Justification of Linkage Size:* To be able to overcome elevated obstacles, the radius of the expanded wheels should be large enough. See Figure 3 for detailed analysis.

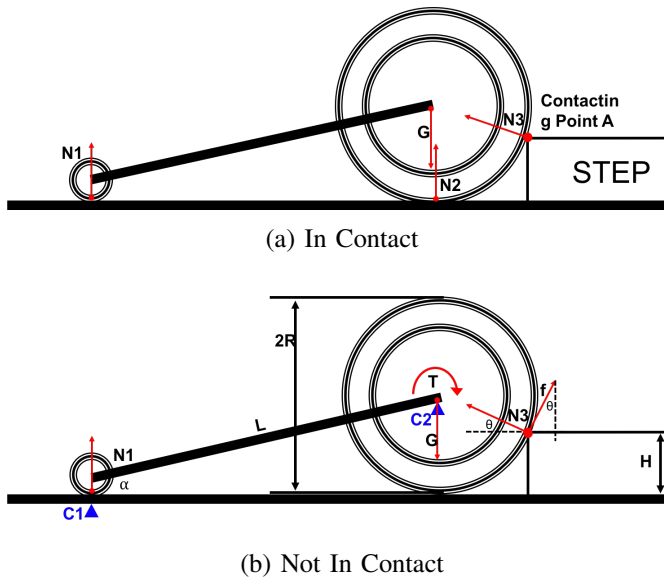


Figure 3: Expanded Mode Wheel Overcoming Elevated Obstacles

As we can see from Figure 3a, the only contacting point between the step and the wheel is Point A. When the wheel is in contact with the ground, there is a normal force  $N_2$  which supports the vehicle. Although the wheel and the step are in contact, normal force  $N_3$  is zero since horizontal components of all forces should be zero, which means

$$\sum F_x = 0.$$

From Figure 3b, the wheel is now lifted and not in contact with the ground. In this case, since the sum of all forces in the vertical direction equals to zero,

$$N_1 - G + N_3 \sin \theta + f \cos \theta = 0, \quad (1)$$

where from the geometry, we know that

$$\tan \theta = \frac{R - H}{H}. \quad (2)$$

Since the sum of horizontal force components also equal to zero,

$$N_3 \cos \theta - f \sin \theta = 0 \quad (3)$$

Now we can use the sum of all the moments about point  $C_1$  equals to zero such that

$$GL \cos \alpha - (N_3 \sin \theta + f \cos \theta)(L \cos \alpha + R \cos \theta) = 0, \quad (4)$$

where

$$\sin \alpha = \frac{R}{L}. \quad (5)$$

Also when consider the moments about point  $C_2$  for the wheel only, we have

$$T = fR. \quad (6)$$

Then from Equation 1 to Equation 5, we can get the relation between the required torque  $T$  and the radius of the wheel  $R$ , which is

$$f = \frac{GL \cos \alpha}{\cos \theta (\tan^2 \theta + 1)(L \cos \alpha + R \cos \theta)}, \quad (7)$$

where we know that  $\theta = \theta(R)$ , and  $\alpha = \alpha(R)$ . And from Equation 7, we can see that as  $R$  increases (Figure 4), the torque required to overcome the step decreases.

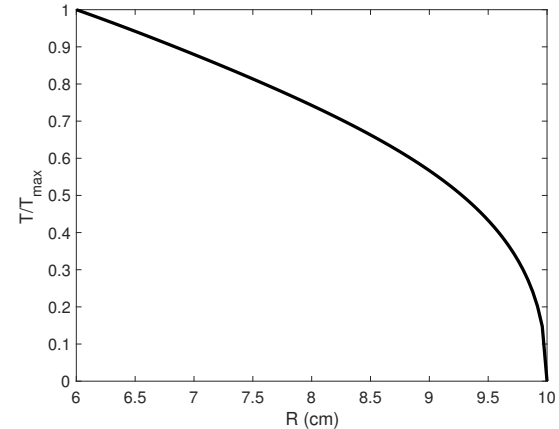


Figure 4: Torque vs. Radius: As the radius of the wheel increases, the torque required to overcome the step decreases. Given a certain motor with a fixed maximum power, we want less torque required so that the time spent on overcoming the step can be decreased due to the increase in rotation speed.

Therefore, for the purpose of overcoming elevated surfaces such as steps, it is ideal that the wheel has a relative large radius. Given the height of the elevated step in the test field is 6 cm, the radius of the expanded wheel should be greater than 6 cm.

However, since there still remains a height limitation on the test field (10 cm). The radius of the wheels in shrink mode should be less than 5 cm.

For the two position analysis, we choose two extreme positions with

$$R_{\text{shrink}} = 40 \text{ mm}, \quad R_{\text{expand}} = 70 \text{ mm},$$

which fit the requirements of the test field.

3) CAD Figures: The CAD drawings for the linkage along is shown in the following figures.

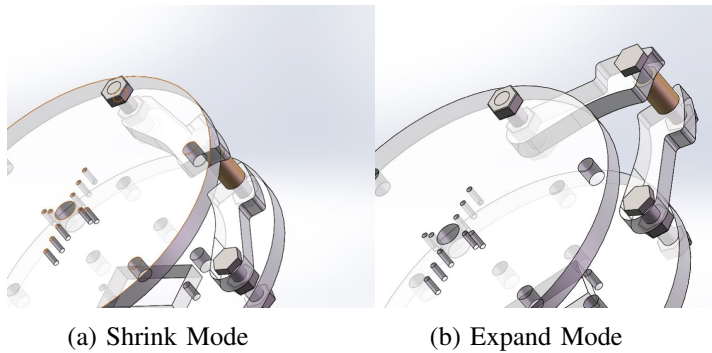


Figure 5: CAD Linkage Drawings

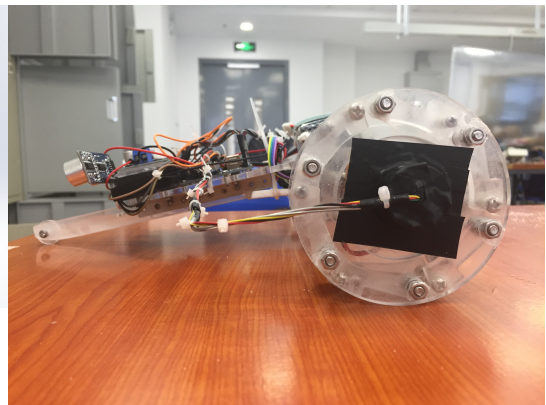


Figure 8: Prototype (Side View)

The CAD drawings for the whole vehicle is shown below.

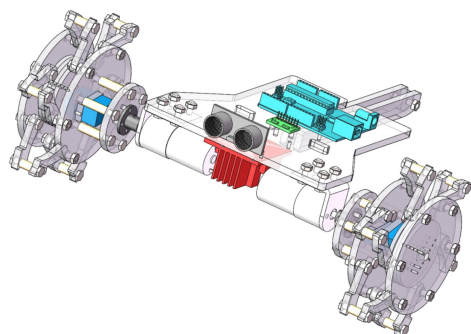


Figure 6: CAD Drawings for Whole Vehicle (subject to assembly modification for the final prototype)

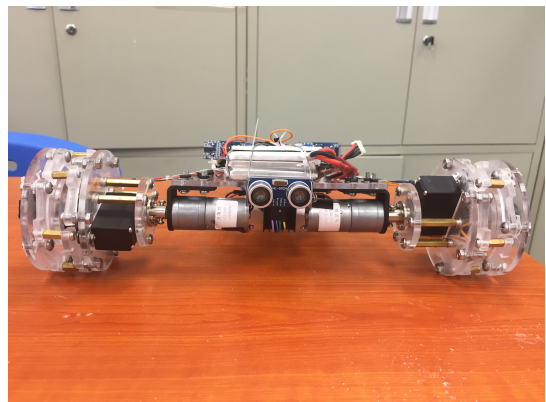


Figure 9: Prototype (Front View)

The detailed part of the vehicles are shown in the following *Assembly* section. And for transformable wheels part, the following figures show it in both shrink and expand mode.

4) *Prototypes:* The completed prototype of the vehicle is shown below.

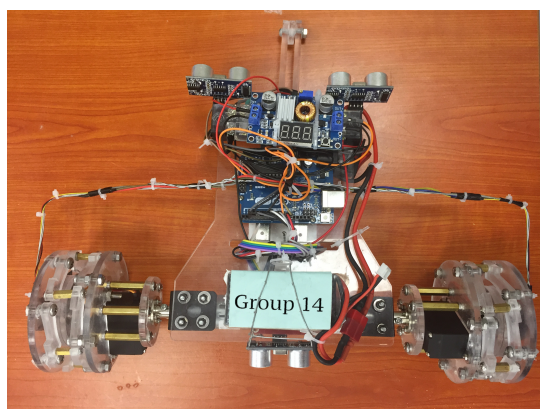


Figure 7: Prototype (Top View)



### (a) Expand Mode

### (b) Shrink Mode

Figure 10: Transformable Wheel Prototype

### III. FABRICATION AND ASSEMBLY

#### *A. Selection of Materials and Components*

*1) Structure:* For the basic structure of the vehicle, we have the following considerations while selecting the materials.

- The structure should be easy to prototype and easy to modify or create a new one if the design of the linkage is modified.
- The basic structure should be light enough since the vehicle (including the mounted electronics) is to be lifted by the servo during wheel transformation.
- The basic structure should also be strong since lots of electronics such as the arduino board, motor controller board, batteries are mounted on the vehicle. Since the vehicle need to climb up and down a step, it will possibly experience force of impact and therefore, the basic structure should be strong.

Upon the listed considerations, we decided to use acrylic board to prototype the basic mechanical structures of the vehicle. Also, we used bolts to serve as the joints between links for the linkage. For the details about how to manufacture and assemble the structure is introduced in the following section.

2) *Electronics:* Since the vehicle is autonomous, it can only rely on sensors to control the motion of the vehicle. Therefore, we choose **Aruidno Uno micro-controller** such that we can input certain programming to the micro-controller for the vehicle to navigate autonomously. (The selection of sensors are explained in the Algorithm section.)

We also have a **motor controller board** to control both motors that actuate the motion of two wheels. The reason to have two motors is that we need to be able to change the proceeding direction of the vehicle since the vehicle can only travel along a field with limited width.

3) *Actuators:* The vehicle needs two kinds of actuators at least to function properly. The first one is motors that allow the vehicle to move forward. The other type of actuator can realize the transformation process. Based on the transformation mechanism design, we choose servos to actuate the transformation mechanism since there are two extreme positions for the transformation process. We can achieve these positions by turning servos to a certain angle. As long as the servo can provide enough torque for the transformation, the transformation process can be completed. And the expand mode of the wheels are held in place by the torque provided by the servo. For the selection of the servo type, we need to first analyze the maximum required torque for the transformation process (See Analysis section for details)

### B. Manufacturing Procedure

After designing the linkage and selection of materials, we first draw the CAD drawings for the structure so that we can get the acrylic board of specific shapes. The drawings for acrylic board is shown in Figure 11.

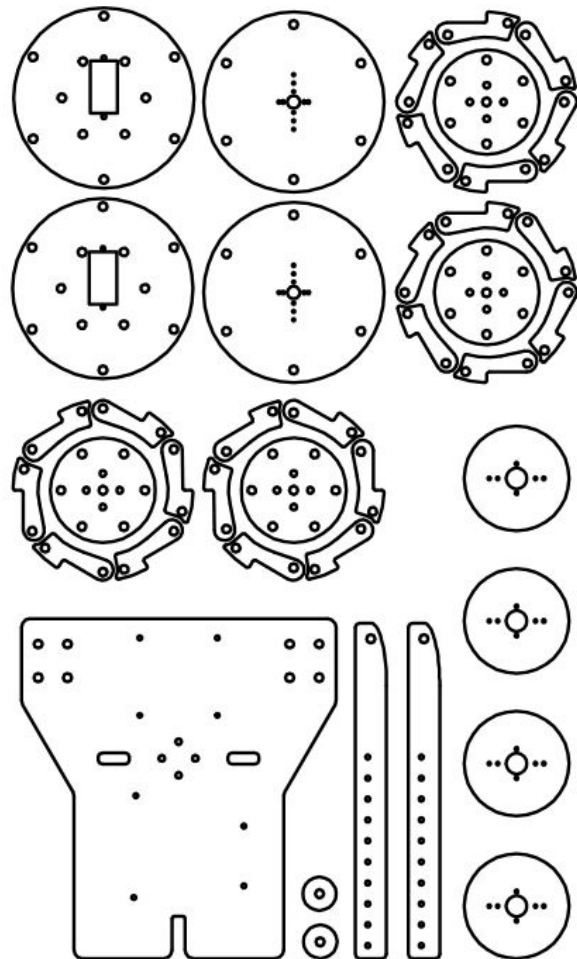


Figure 11: CAD Drawings for Acrylic Board

Since the acrylic structure of the vehicle is the only part that needs to be manufactured to certain shapes, once the acrylic structure is manufactured, we can enter the assembly process.

### C. Assembly Procedures

The assembly process is divided into three parts: transformable wheels, body structure and arrangement of wires.

1) *Transformable Wheels:* The main part of wheels is acrylic board (semitransparent material in Figure 12) connected with screws, nuts and copper pillars (yellow cylinder in Figure 12). Other components include a servo (blue block in Figure 12) and a flange coupling (black columnar structure in Figure 12).

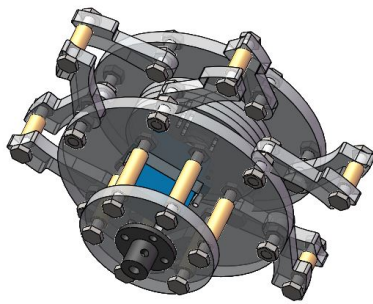


Figure 12: Overview of the Transformable Wheel

As shown in Figure 13, the rectangle hole is designed for placing the servo. Then the servo is covered by a circular board connecting flange coupling. The two pieces of acrylic board are connect by M4×16mm copper pillars.

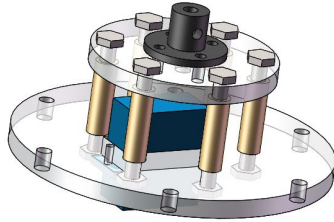


Figure 13: Servo Part of Transformable Wheel

On the other side of the servo, as shown in Figure 14, six teeth are attached to the big circular board with M4 screws and nuts. The connection should not be too tight, otherwise the friction will be very large. Lubrication oil may be needed. Above the teeth, there are six M4×10mm copper pillars (yellow cylinder in Figure 14).

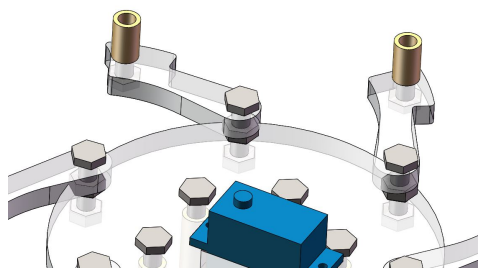


Figure 14: Other Side of Transformable Wheel

Till now, only half of the tooth is completed. The other side of the tooth is assembled in the same way but in counter direction, as shown in Figure 15. After the six teeth are done, the last circular board is then placed above the teeth. This board is also connected to

the rotating paddle of the servo (not drawn in the figure), in which case, the two big circular board can have angle difference due to the rotation of servo paddle. Then the assembling of wheels is finished.

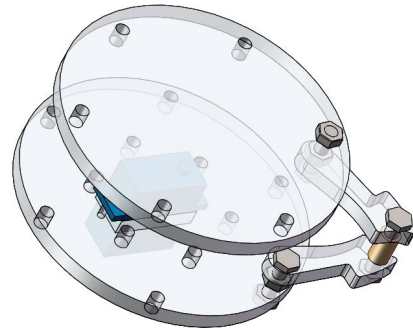


Figure 15: Whole Tooth of Transformable Wheel

*2) Body Structure:* The floor panel of the vehicle is also a piece of acrylic board, with a tail. The tail is a small circular board sandwiched by two long strip boards, as shown in Figure 16. This is the back wheel of the vehicle, and it is fixed by one M4×18mm screw. The tail can be simply stuck onto the floor panel. An L-type angle iron is a better choice. Two motor brackets (while L shaped block in Figure 16) are fixed on the front part of the floor panel by screws and nuts. Then we can install the motors onto the brackets.

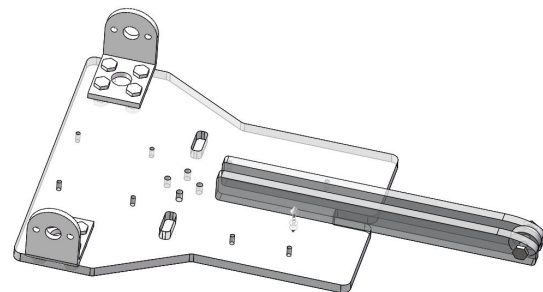


Figure 16: Floor Panel of the Vehicle

Figure 17 is the bottom side of the vehicle. After the two motors are installed, the driven board L298N (red block in Figure 17) is fixed between the two motors. L298N should be a good match for the room between the two motors. Then the two wheels can be installed to the shafts of the motors.

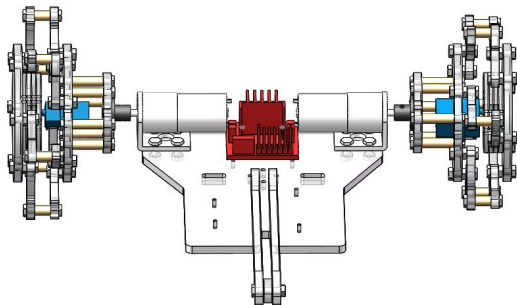


Figure 17: Bottom Side of the Vehicle

Then on the upper side of the vehicle, the MPU6050 Model (green block in Figure 18), the HC-SR04 Model (gray block in Figure 18) and arduino uno board (cyan block in Figure 18) are fixed by screws and nuts. The vehicle should be like what is shown in Figure 18. The battery (not shown in the figure) can be stuck onto the upper side. Then the whole structure is completed.

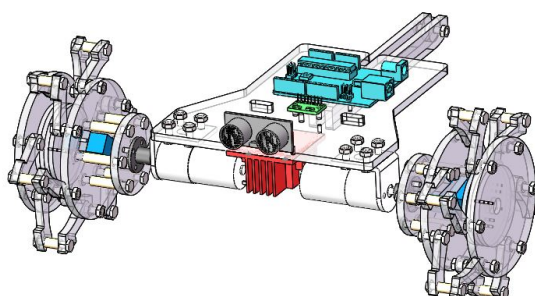


Figure 18: Overview of the Vehicle

*3) Arrangement of Wires:* Wire Connection for HC-SR04 Model is shown in Figure 19.

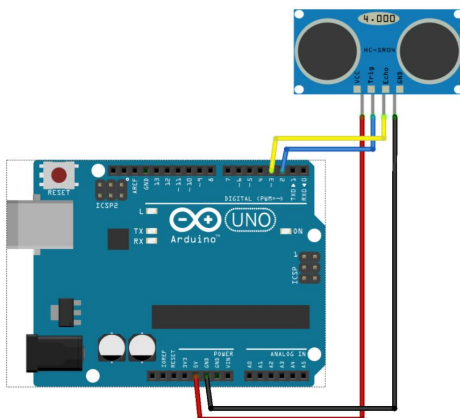


Figure 19: Wire Connection For HC-SR04 Model

Wire Connection for MPU6050 Model is shown in Figure 20.

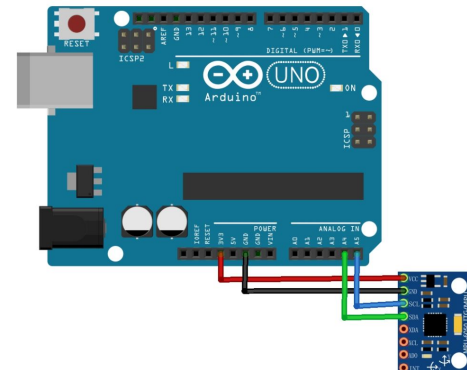


Figure 20: Wire Connection For MPU6050 Model

Wire Connection for two motors and the driven board L298N is shown in Figure 21. The red and black lines should be connect to the positive and negative end of battery (not shown in the figures) directly.

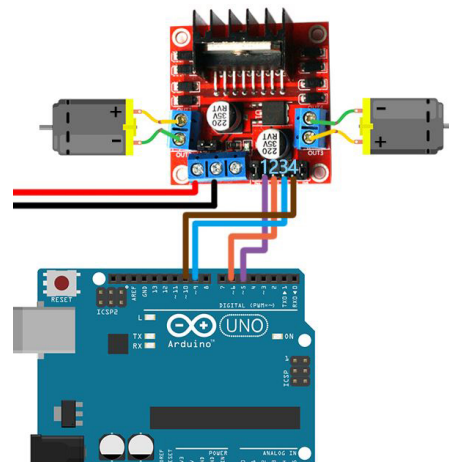


Figure 21: Wire Connection For L298N

Wire connection for servo is shown in Figure 22. The two servos work at the same time, so they can share one signal pin on arduino board.

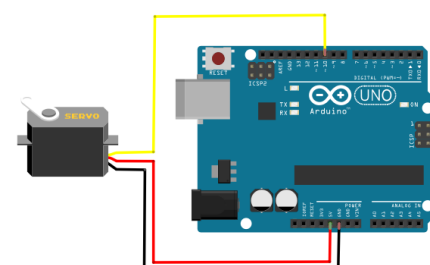


Figure 22: Wire Connection For Servo

On the floor panel of the vehicle, there are some holes designed for wires arrangement. One thing to mention is that all the electronic devices should be grounded together.

#### IV. ALGORITHM ON THE PROGRAMMING FOR SENSORS

##### A. HC-SR04 Model

HC-SR04 Model uses ultrasonic wave to detect the distance between the sensor and the obstacle. One HC-SR04 Model is placed in the front of vehicle to detect the distance between the vehicle and the wall of the sand box. When the distance is smaller than 5cm, the wheels transform from the shrink mode to the expansion mode. Another two HC-SR04 Models are placed at the both sides of vehicle to detect the distance between the sides of the vehicle and the walls of the game field. If the distance between a wall and vehicle is smaller than 5cm, the rotational speed of the wheel that is away from the wall will decrease so that the vehicle will move away from the wall. We used loop in Arduino code so that the distances between the walls and vehicle was detected every 3 seconds.



Figure 23: HC-SR04 Model.

##### B. MPU6050 Model

We utilized pitch of MPU6050 Model to detect whether the vehicle has climbed on the sand box and whether the vehicle has run off the sand box. If pitch is larger than 20, the vehicle has climbed on the sand box. If pitch is smaller than 20, the vehicle has climbed off the sand box. When the vehicle has run off the sand box, the wheels transform from the expansion mode to the shrink mode.



Figure 24: MPU6050 Model.

##### C. Flowchart

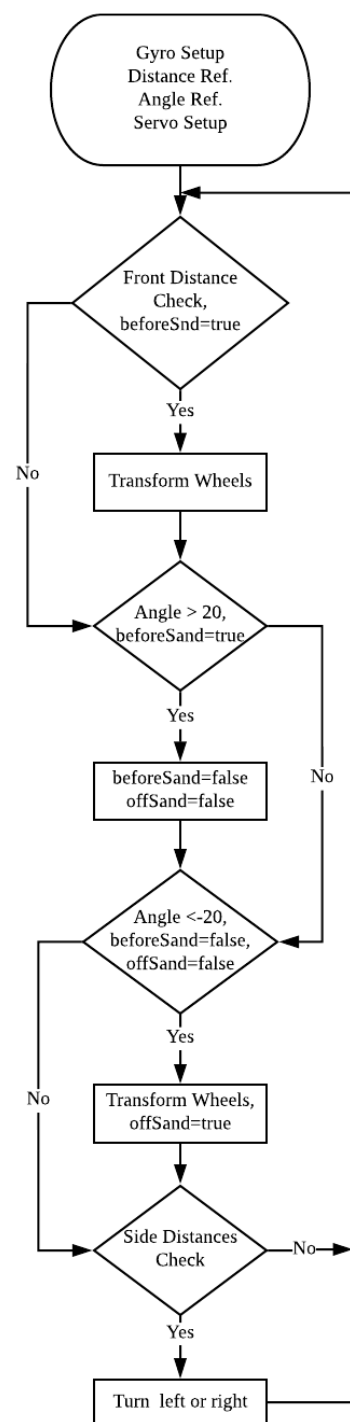


Figure 25: Flowchart of algorithm on the programming for sensors.

## V. ANALYSIS

### A. Classification of the Designed Linkage

Since the linkage of the transformation mechanism is a four-bar linkage. The mobility (degree of freedom) of

the linkage is 1. One of the six identical four-bar linkage is annotated in the following figure.

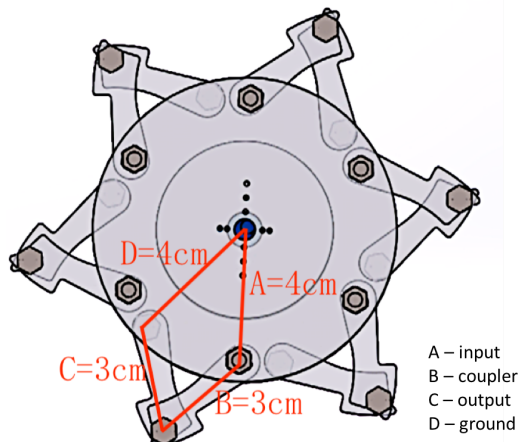


Figure 26: Four-bar Linkage of the Transformable Mechanism

And as we can see from Figure 26, the input and the ground linkage is both 3 cm and the coupler and the output linkage is both 4 cm. Given the Grashof condition,

$$S + L = P + Q, \quad (8)$$

we can conclude that it is a **Special Case Grashof Linkage: SC Double Rocker (SRCR)**.

### B. Transformation Position Analysis

There are two extreme positions that we designed for the transformation. Since before and after the transformation, the wheels will be rotating on a *effective radius* that is determined by the mode of the wheel. The schematic of six identical linkages in the transformation mechanism is shown below.

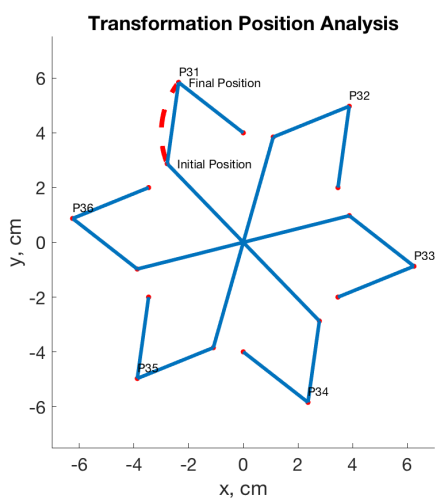


Figure 27: Six Identical Linkage in the Transformation Mechanism

In Figure 27, the red dashed line shows a trajectory of a point on the *effective radius* that will be in contact with the ground during motion. By calculation, the radius change of the *effective radius* is from 3 cm to 6.3 cm while the input linkage will be rotating from an input angle  $\theta = 88^\circ$  to  $\theta = 44^\circ$ . The difference between the linkage analysis result and the final prototype linkage transformation will be discussed in the Experiment part in detail.

### C. Force Analysis

The maximum torque that is required is when the transformation begins. The following figure shows the schematic of the wheel that begins transformation (in shrink mode).

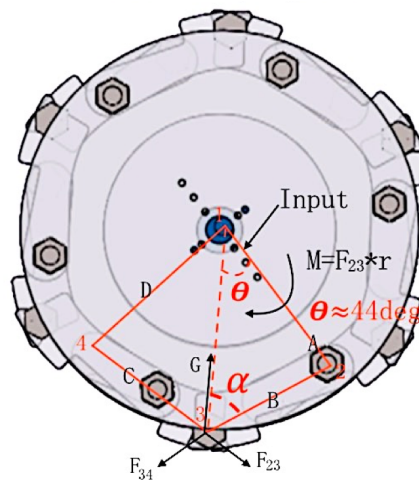


Figure 28: Initial Maximum Torque Position

As we can see from Figure 29, we assume that during transformation, there is only one linkage that is in contact with the ground while in fact there will be two linkages in contact. By assuming this transformation geometry, we proceed to analyze the required torque for transformation.

As we can see at the contacting point, since the output and the coupler is of the same length. The forces that apply to both linkages are the same. ( $F_{23} = F_{34}$ ) Note that the red dashed line in the figure is the *effective radius*  $L$  of the wheel. Consider the triangle that is enclosed by the *effective radius*, the output linkage and the coupler, we have

$$\frac{\sin \alpha}{A} = \frac{\sin \theta}{B} = \frac{\sin(\alpha + \theta)}{L}, \quad (9)$$

where  $L$  is the length of the *effective radius*,  $\theta$  is the angle between the ground and the input linkage and  $\alpha$

is  $1/2$  of the angle between the coupler and the output. Then we have,

$$\alpha = \arcsin \left( \frac{A \sin \theta}{B} \right), \quad (10)$$

$$L = \frac{B \sin(\alpha + \theta)}{\sin \theta}. \quad (11)$$

Then for the forces, we have

$$2F_{23} \cos \alpha = G, \quad (12)$$

where  $G$  is the  $1/2$  weight of the vehicle for one wheel, which we assume that  $G \approx 0.7$  kg. Then the torque required can be calculated by

$$M = F_{23} L \sin \alpha, \quad (13)$$

where we have assumed that the output and coupler forms a right angle ( $90^\circ$ ). The relationship between the required torque to hold the linkage at a angle of  $\theta$  is shown in the following figure, where  $\theta$  is  $1/2$  of the input angle.

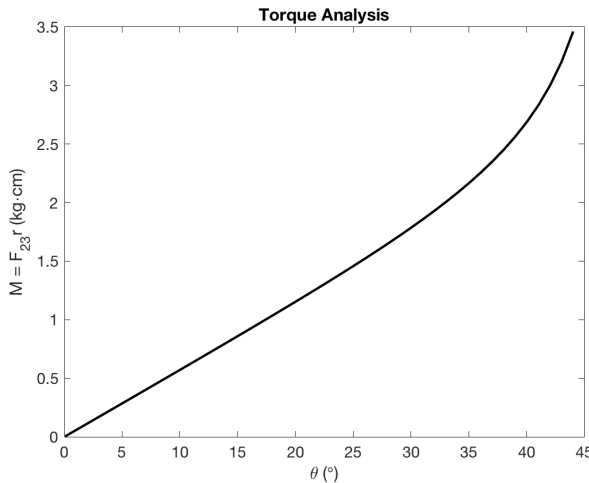


Figure 29: Required Torque at Input Angle of  $2\theta$

As we can see from Figure 28, the maximum required torque  $M_{max} \approx 3.5$  kg · cm.

Given that the servo we select has a maximum input torque of  $M_{servo,max} = 13$  kg · cm. The servo should have enough torque to transform the wheel.

#### D. Rolling Speed Analysis

Based on the design of the wheel, we need to analyze two kinds of rolling speed, both under the assumption of **non-slip** condition when in contact of the ground.

1) *Shrink Mode*: For the shrink mode, the motion of the wheel can be modeled as a circle in contact with a

flat plate. Assume we have motor speed  $\omega$  and a radius of  $r$ . Then the rolling speed of the wheel is

$$v_{shrink} = \omega r, \quad (14)$$

where  $r$  is the radius of the wheel that is in shrink mode, which is 40 mm. And the motor speed of our choice is  $60$  rpm =  $2 * \pi$  rad/s. Then we have a shrink rolling speed of

$$v_{shrink} = 4 \text{ cm} \times 2\pi \text{ rad/s} \approx 25 \text{ cm/s}.$$

2) *Expand Mode*: For the expand mode, the rolling process of the wheel can be divided into individual intervals that is a rotation about the contacting point for  $\beta = 60^\circ$ . The following diagram shows the rolling process of a expand wheel.

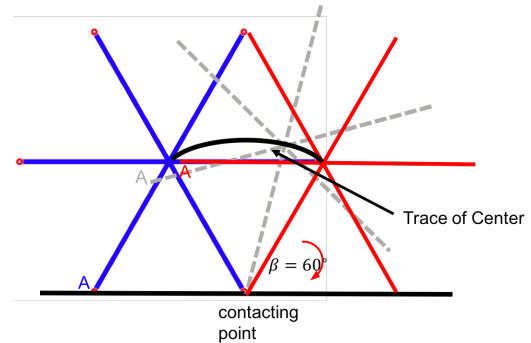


Figure 30: Rolling Process of a Wheel in Expand Mode

In Figure 30, the six spikes all have the radius of the maximum *effective radius* of  $r = 6.3$  cm by calculation. For one full revolution of the wheel, it will experience six intervals which is shown in the figure. When we evaluating the rolling speed of the wheel, we will measure the average speed of the center of the wheel moving forward. Therefore, the rolling speed of the vehicle can be calculated by

$$v_{expand} = r/t = \frac{r}{\pi/6/\omega} \approx 75 \text{ cm/s}, \quad (15)$$

where  $\omega$  we used is the rotating speed of the motor itself. But this may differ from real case a lot.

But by simple comparison, we can see a large increase in rolling speed of the wheel when it is in expand mode.

#### E. Study of Number of Teeth

We wonder whether changing number of teeth can affect the performance of transformable wheels. With the same two position synthesis condition, if we change the number of teeth, the length of the links also change. We fix the length of OA=4cm in Figure 31. We want the diameter of wheel does not change in expand mode,

namely length of OB stay the same as that in our origin design. Then we can determine the length of AB (denoted by x).

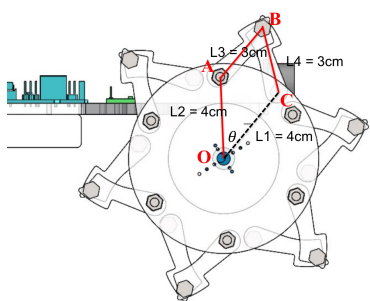
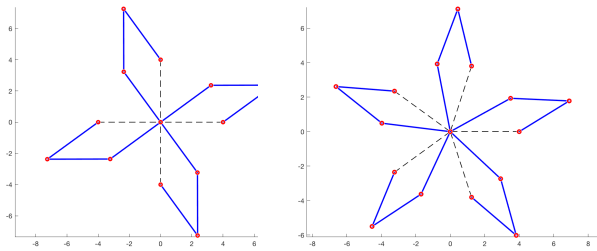
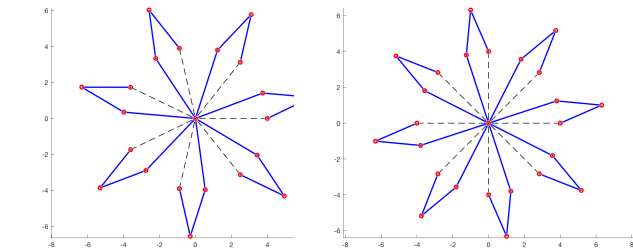


Figure 31: Four-bar Linkage Dimension

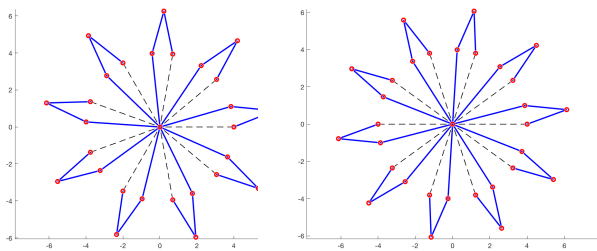
We find that length of AB (x) decreases with the increase of the number of teeth, as shown in the following table.



(a) Number of Teeth n=4 (b) Number of Teeth n=5



(c) Number of Teeth n=7 (d) Number of Teeth n=8



(e) Number of Teeth n=9 (f) Number of Teeth n=10

Figure 32: Different Number of Teeth

Length of AB [cm]	4.0	3.4	3.0	2.7	2.5	2.4	2.3
Number of Teeth n	4	5	6	7	8	9	10

Table I: Change of x with the Number of Teeth

Similarly, we study the torque required in each case. When rotating angle increases from 0 to  $2\pi/n$ , the torque required increase first and then decreases. This is because the wheel is at shrink mode at 0 and  $2\pi/n$ . The maximum torque occurs at the expand mode Let us denote the rotating angle by  $\theta_{max}$  at expand mode. From Figure 33, we find that the maximum input angle  $\theta_{max}$  decreases as n increase. This is to say, if we use more teeth, the angle displacement of driven servo is smaller, and thus the time needed to transform will be reduced.

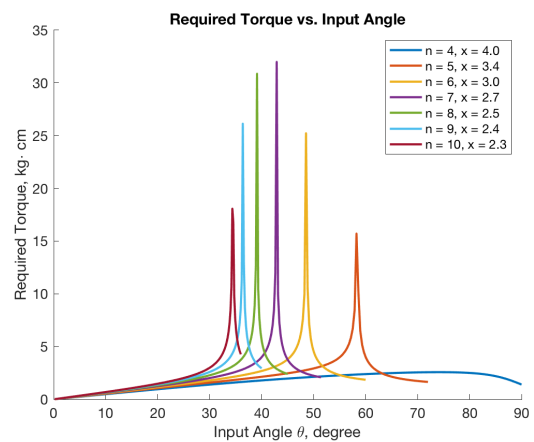


Figure 33: Required Torque for Different Number of Teeth

Since we also want the maximum torque to be as small as possible, n=4 seems to be a good choice. However, in reality, the less the number of teeth is, the less stable the system will be. This is because if the number of teeth is too less, the vibration of the vehicle will be too large. The links may break because of the impact. When n>7, as the number of teeth increases, the maximum torque also decreases. However, we can not get the conclusion that the larger n is, the better the wheel will be. This is because when n increases, the friction in the joints becomes not negligible. In Figure 31, we do not take the friction into consideration because it is small compared with the self weight of the vehicle. In Figure 31, the maximum torque at n=6 is smaller than n=7,8,9, we may conclude that n=6 is a better design. Without considering the friction and cost of manufacturing, large n(>9) improves the performance of transformable wheel. We also think that n=5 can be a better choice than n=6. The curve at n=5 is similar to others, unlike n=4, so we can consider n=5 as a design of reaching small torque

by sacrificing stability to some degree. More text need to be applied to verify our guess.

## VI. EXPERIMENT

### A. Demonstration of load caring capacity

We gradually added loads on our vehicle, and stopped when the wheel failed to completely expand. Figure 34 was taken when vehicle completed transformation with the maximum loads. We measured both the mass of loads, which was 1.39 kg, and the mass of vehicle itself, which was 1.10 kg. So the loading caring capacity of our vehicle was 2.49 kg.

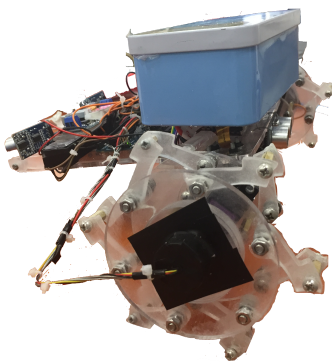


Figure 34: Vehicle with Loads in the Expansion Mode of Wheel.

Theoretically, the load caring capacity of the vehicle is 2.74 kg. In Figure 29,  $A=D=4$  cm,  $B=C=3$  cm, and  $\theta$  changes from  $43.5^\circ$  to  $21.5^\circ$ . The maximum torque applied by the servo is  $M=13$  kg·cm.

$$\begin{aligned}\alpha &= \arcsin(A \sin \theta / B) \\ L &= B \sin(\alpha + \theta) / \sin \theta \\ r &= L \sin \alpha \\ F_{23} &= M/r \\ G &= 2F_{23} \cos \alpha\end{aligned}$$

Using the above equations, we calculated the load capacity of the vehicle to be 2.74 kg. The actual load caring capacity is a little smaller than the theoretical value due to the friction forces. When we test the maximum load, we find that if we change the position of the load, the test results are different. The results we report are all reached under the condition that the barycenter of the load is above the two transformable wheels. Based on this discovery, we can improve the design by moving the barycenter of the vehicle backwards.

### B. Demonstration of climbing onto the sand box and running through the tunnel

We used the expand mode of the wheel to climb onto the sand box. Figure 35 shows that the vehicle climbed onto the sand box.

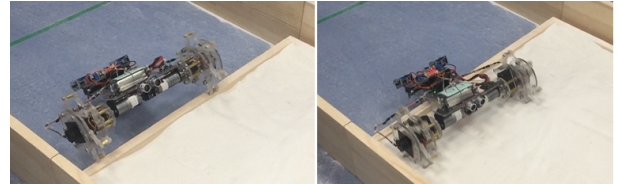


Figure 35: Vehicle climbed onto the sand box.

We used shrink mode to run through the tunnel. Figure 36 shows that the vehicle ran through the tunnel.

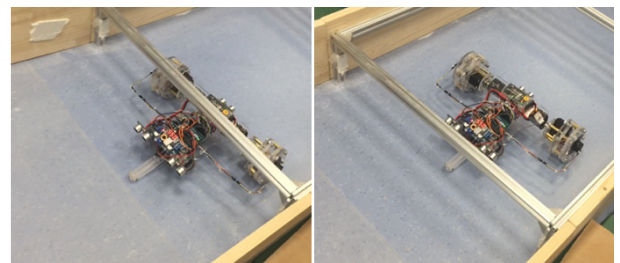


Figure 36: Vehicle ran through the tunnel.

### C. Demonstration of rolling on sand and smooth surface

When the wheels were in shrink mode and ran on the smooth surface, we recorded the time that the vehicle needed to run through the tunnel. The time was 2.56 s, and the length of the tunnel was 60 cm. The speed of the vehicle was measured to be 23.44 cm/s. Since the diameter of the wheels in shrink mode was 8.6 cm, the rotational speed of the wheels was 5.45 rad/s (52.04 rpm). Theoretically, the rotational speed of the wheels is 60 rpm at both shrink mode and expansion mode. The rotational speed of shrink mode wheel on smooth surface was slightly smaller than the theoretical value. The theoretical value is the rotational speed of wheel with zero load and zero friction force. However, the mass of the vehicle was 1.10 kg, and there existed friction forces between the wheels and the surface. Moreover, there were friction forces between the connection parts of the motors and wheels. So there were torques on the wheel due to the friction forces. Therefore, for the same output torque of the servo motor, a part of the output torque was used to overcome the torques caused by friction forces, and the rotational speed of wheels was decreased.

When the wheels were in expansion mode and ran on the smooth surface, the rotational speed of the wheels

was measured to 57.69 rpm. It was slightly smaller than 60 rpm. When the wheels were in expansion mode, not only the friction forces caused torque on the wheel, but also the weight of vehicle. After an expansion leg started contacting the surface, the contact point of the wheel and the surface moved backward as the vehicle moved forward until another expansion leg touched the surface. As one expansion leg started touching the surface, the torque caused by vehicle weight first decreased and then increased until the leg left the surface. The rotational speed was thus first increased and then decreased. So the rotational speed of the wheel of expansion mode were not constant, but varied. The average rotational speed was smaller than the theoretical value due to the torque of friction forces between wheels and surface, vehicle weight, as well as the friction forces between the connection parts of motors and wheels.

When the wheels were in expansion mode and ran on the sand, we measured the time that the vehicle ran through the sand box. The time was 2.52 s, and the length of the sand box was 60 cm. The speed of vehicle on the sand was 23.81 cm/s. At the expansion mode, the diameter of the wheels was 14 cm. The rotational speed of the expansion wheels on sand was thus 3.54 rad/s (33.82 rpm), which was smaller than theoretical value of 60 rpm. The reasons discussed for wheel in expansion mode on smooth sphere also applied here. However, the rotational speed of wheels in expansion mode on the sand was much smaller than that of wheels in expansion mode on smooth surface. This was because the grains of sand were very small and had rough surfaces. The friction coefficient became larger. So the friction force between the wheel and sand were much larger than that between the wheel and the smooth sphere. Torque caused by the friction force was therefore larger. This led to that the rotational speed of the expansion wheels on sand was much smaller than that of expansion wheels on smooth surface. The surface of the sand was not flat, so the actual distance that the vehicle traveled in sand box was larger than 60 cm. The actual rotational speed of the wheels in expansion mode on sand might be larger than 33.82 rpm.

#### D. Demonstration of Transformability

The diameter of wheel in the shrink mode was measured to be 8.6 cm, and the diameter of wheel in the expansion mode was 14.0 cm. The increase in the diameter of wheel after transformation was thus 5.4 cm. Theoretically, after wheel transformation, the input link rotates 44°, and the diameter of wheel in expansion mode is 14.9cm. The real diameter of wheel in expansion

mode was smaller than the theoretical value due to the vehicle weight. The support force exerted from the surface added a counterclockwise torque on the input link. The steering engine applied clockwise torque to hold the input link in place. So a part of the output torque of the steering engine was utilized to counteract the external torque. Therefore, the input link rotated an angle slightly smaller than 44°, and the diameter of wheel was a little decreased.

## VII. DISCUSSION

### A. Agreement and disagreement with previously published work

In the paper named "Wheel Transformation: A Wheel-Leg Hybrid Robot With Passive Transformation Wheels", the authors used three pin-slot linkages, 120° apart, to retract and to stretch out three legs in a circular wheel. The authors used pin-slot four-bar linkages to realize wheel transformation. We also used four-bar linkages to transform wheel, but the linkage type was special case III. We used special case III linkage so that when the wheel was in expansion mode, the support force given by the surface was decomposed by coupler link and output link. Compared with the design in the paper, for our vehicle, the links that contacted the ground bore smaller forces. Moreover, we used six four-bar linkages in a wheel instead of three as the authors did. We used six linkages in a wheel so that the wheel needed to rotated at most 60° to climb onto the wall of the sand box. Also, when a leg started contacting the ground, the angle between the leg and the vertical central line of the wheel was 30°. This angle was designed to be small to limit the maximum external torque exerted on the input link and the external torque on the servo motor.

### B. Theoretical and practical implication of our work

Our work has proved that six special case III linkages in a wheel can accomplish wheel transformation so that the vehicle can run on different surfaces including smooth surface and sand, and can climb over a wall with certain height. We have provided a feasible method for those who will later study transformable wheel. In practice, our work can be applied in rescue operations. For instance, if many building fall down during the earthquake, our vehicle will efficiently enter the collapsed buildings to look for persons trapped there. Usually the gaps between the broken bricks are too small to enable a rescuer to get through. It takes hours to expand a gap to let a person get through, but it takes little time to expand a gap to enable a small vehicle to get through. Instead of wasting time removing the bricks to see if there is

living person inside, our vehicle can immediately get in the collapsed building, and run on the rough surfaces in expansion mode and on smooth surface in shrink mode to search through the whole space in a short time. With the sensors we used on our vehicle, the vehicle can avoid bumping into obstacles, and transform accordingly. Using our vehicle can detect living persons trapped in collapsed building in a short time, and improved the efficiency of rescue operations so that more persons can be saved.

### VIII. CONCLUSION

#### A. Objectives and Methods

In this project, we need to design a vehicle with transformable wheels to accommodate the different surfaces or to overcome obstacles. We simulate different situations that vehicles may encounter, including a 6cm height step(obstacles), sand(desert) and concrete land(road), 10cm height gate(tunnels). High stability and also high speed are the two most important factors to evaluate the performance of the design.

We designed a six-teethed transformable wheel to make the vehicle climb or pass through the obstacles stably and fast. Our design is based on special case III four-bar linkage, which transforms angle displacement into change in diameter.

#### B. Key Findings List

- 1) If we use more teeth, the angle displacement of driven servo will be smaller, and thus the time needed to transform will be reduced.
- 2) The maximum torque required increases first and then decreases as the number of teeth increases.
- 3) Changing the number of teeth and moving the barycenter backwards can improve the performance of transformable wheels.

### REFERENCES

- [1] Lee D, Kim J, Kim S, Koh J, Cho K. "The Deformable Wheel Robot Using Magic-Ball Origami Structure," *ASME. International Design Engineering Technical Conferences and Computers and Information in Engineering Conference, Volume 6B: 37th Mechanisms and Robotics Conference ()*:V06BT07A040.
- [2] Laney D, Hong D. "Three-Dimensional Kinematic Analysis of the Actuated Spoke Wheel Robot," *ASME. International Design Engineering Technical Conferences and Computers and Information in Engineering Conference, Volume 2: 30th Annual Mechanisms and Robotics Conference, Parts A and B ()*:933-939.
- [3] Yu She, C. J. Hurd and H. J. Su, "A transformable wheel robot with a passive leg," *2015 IEEE/RSJ International Conference on Intelligent Robots and Systems (IROS)*, Hamburg, 2015, pp. 4165-4170.

- [4] Y. Kim, G. Jung, H. Kim, K. Cho and C. Chu, "Wheel Transformer: A Wheel-Leg Hybrid Robot With Passive Transformable Wheels," in *IEEE Transactions on Robotics*, vol. 30, no. 6, pp. 1487-1498, Dec. 2014.
- [5] Yun, Sung-Sik. Lee, Jun-Young. Jung, Gwang-Pil. Cho, Kyu-Jin. "Development of a transformable wheel actuated by soft pneumatic actuators", *International Journal of Control, Automation and Systems*, 15(1), Jan. 2017.



**Xuesong Ren** Junior student in Joint Institute, Shanghai Jiao Tong University.



**Changqing Lu** Junior student in Joint Institute, Shanghai Jiao Tong University.



**Rui Chen** Junior student in Joint Institute, Shanghai Jiao Tong University.



**Muwei Teng** Junior student in Joint Institute, Shanghai Jiao Tong University.

**APPENDIX A**  
**LITERATURE REVIEW**

The followings are the literature related to transformable wheels that we have reviewed and analyzed for their advantages and disadvantages.

No.	Method	Major findings	Unresolved Issues	Refs.
2006 (DETC) Virginia Tech - 3D kinematic analysis of spoke wheel robot	Actuated Spoke Wheel	Kinematics of a vehicle with two actuated spoke wheels are analyzed in both straight-line walking and steady state turning states.	Vehicles will generate sudden accelerations due to rapid motion change. Wheels are not transformable. No slip and no bounce constraints at the contact points are ideal for actual applications.	[2]
2013 (DETC) SNU - Deformable wheel robot using magic ball origami structure.pdf	Magic Ball Origami Structure	Origami inspired transformable structure can be applied into manufacturing transformable wheels. Able to pass through height-limited tunnel.	Manufacturing complicated and difficult. Transformed shapes were not proved to be able to overcome elevated obstacles.	[1]
2014 (IEEE) SNU - Wheel transformer.pdf	Pin-slot linkage	Three pin-slot linkages, 120° apart, in a wheel enables three legs to retract in the circular wheel and to stretch out to form a legged wheel.	Control of the phases of two wheel during wheel transformation to prevent the vehicle from tilting laterally.	[4]
2017 (IJCAS) SNU - Transformable wheel actuated by pneumatic actuators.pdf	Soft pneumatic actuator	Utilizing soft pneumatic actuators to emerge legs from the circular wheel can transform wheel under a high payload.	The effect of buckling in performance of soft pneumatic actuator cannot be predicted.	[5]
2015 (IEEE) Ohio State - Transformable wheel robot with a passive leg.pdf	Slider-crank Linkage with Passive Leg	Slider-crank linkage enables transformation. Passive leg embedded to decrease the actuation force for transformation.	Difficulty in identifying the transformation position with the passive leg supporting the load.	[3]
	Four-bar Linkage	Smooth wheel transformation with four-bar linkage.	Relative high actuation force of transformation.	Proposed Work

**APPENDIX B**  
**GANTT CHART, TOGETHER WITH THE CONTRIBUTION OF TEAM MEMBERS**



Figure 37: Project Plan

**APPENDIX C**  
**BUDGET AND JUSTIFICATION**

Item	Product or Materials	Quantity	Unit Price (RMB)
1	Motor	2	22.0
2	MG996R Servo	2	23.5
3	Acrylic board	1	79.0
4	Screws, nuts and connecting pieces	/	50.0
5	Arduino UNO Board	1	74.0
6	L298N Driven Board	1	12.0
7	LM2596 DC-DC Depressurization Module	1	12.0
8	Slip Ring	2	23.0
9	Flange coupling	2	11.0
10	Sensors	2	40.0
11	Wires	2	10.0
Total			436.0 (RMB)

Table II: Budget

The total cost is under budget.